Journal of Radioanalytical and Nuclear Chemistry
https://doi.org/10.1007/s10967-022-08215-2

Direct uranium enrichment assay in gaseous uranium hexafluoride with laser induced breakdown spectroscopy

George C.-Y. Chan[1] · Xianglei Mao[1] · Leigh R. Martin[2] · Lee D. Trowbridge[2] · Richard E. Russo[1,3]

Received: 5 November 2021 / Accepted: 20 January 2022

Abstract

A set of eleven U atomic emission lines, between 421.099 and 421.460 nm, were characterized for direct enrichment assay of gaseous UF_6 samples with laser induced breakdown spectroscopy (LIBS). Several iterative, multivariate nonlinear spectral-fitting algorithms were evaluated for their efficacies to extract the enrichment information from the measured LIBS spectra. Wavelength-dependent weight factors, which take into consideration of the spectral-line position in the fitting model, the determined isotopic ratio, and the isotopic shift of the emission line, are essential for the spectral-fitting model to function adequately. The analytical accuracies and precision were typically within 0.5% in absolute [$^{235}U/(^{235}U + ^{238}U)$] ratios.

Keywords Uranium hexafluoride · Enrichment assay · Isotopic analysis · Isotopic shift · Laser induced breakdown spectroscopy

Introduction

Uranium is considered as a dual-use element in the community of nuclear safeguards and security because it can be used for peaceful civilian as well as military purposes. Natural uranium (NU) contains around 0.72-atom% of ^{235}U, 99.27-atom% of ^{238}U, and a trace amount of ^{234}U in secular equilibrium with ^{238}U [1]. In almost all nuclear applications, the abundance of the fissionable ^{235}U is too low in NU, and thus, ^{235}U enrichment is needed. The enrichment level depends on the specific application and is typically a few percent for civilian use [2, 3]. Uranium enrichment is a concern for safeguards. For enrichment, uranium is first transformed to UF_6—the only known volatile compound of uranium [4]—and enrichment is then performed almost exclusively by gaseous diffusion or centrifuge process [2, 3]. As the first line of defense against proliferation, accurate UF_6 enrichment assays are critical for materials verification, accounting and safeguards. In addition, fieldable analysis is highly desirable because sample shipment to an off-site laboratory is costly and cumbersome in logistics, and results are not available without delay after sample collection [5].

Recently, several optical-based analytical techniques for performing U isotopic analysis in the field have been reported [6–13]. For example, high-resolution infrared spectroscopy [6–9] probes the rotational-vibrational transitions in gaseous UF_6 molecules. In this case, enrichment assay is based on the isotopic shifts between the $^{235}UF_6$ and $^{238}UF_6$ vibrational frequencies. The electronic transitions between ^{235} and ^{238}U atoms also exhibit appreciable isotopic shifts useful for isotopic analysis. For instance, wavelength tunable diode lasers, which are capable of delivering narrow line width and hence high spectral resolution, are used for U isotopic analysis through atomic absorption [14–16]. Spectral resolution can be further enhanced through the use of atomic beam laser absorption spectroscopy, as demonstrated by Castro and co-workers [10, 11]. Through a small aperture located at the exit of a resistively heated micro-oven [17], the expansion of the free U atoms is highly directional (i.e., atomic beam) and consequently reduces atomic line width and the likelihood of spectral interference.

Laser induced breakdown spectroscopy (LIBS) is a demonstrated fieldable technique [18, 19] for elemental analysis. The isotopic shifts of some of the U atomic emission lines are large enough to be at least partially resolved in this

✉ George C.-Y. Chan
gcchan@lbl.gov

[1] Lawrence Berkeley National Laboratory, Berkeley, CA 94720, USA

[2] Oak Ridge National Laboratory, Oak Ridge, TN 37830, USA

[3] Applied Spectra, 950 Riverside Pkwy Suite 90, West Sacramento, CA 95605, USA

plasma emission source operated under atmospheric pressure [12, 13, 20, 21]. In this context, the term "atoms" collectively refer to neutral atoms or atomic ions. In one of our previous studies [12], we reported an analytical and multivariate nonlinear spectral processing method for the extraction of U isotopic information of the sample from the acquired LIBS spectra in the wavelength range of 424.3–424.5 nm. Extraction of isotopic information with spectral fitting does not require the use of isotopically enriched standards for calibration. The spectral-fitting method was tested with a set of solid U-bearing glassy disks with ^{235}U enrichment ranging from natural to highly enriched levels (~94%), and the reported accuracies (biases) were within ± 1% and precisions were about 0.2% in the absolute [^{235}U / (^{235}U + ^{238}U)] ratios [12]. In follow-up work [13], the method was tested directly on gaseous UF_6 samples. However, systematic positive biases were found for UF_6 enrichment assays performed with the ^{235}U–^{238}U line pair at 424.412–424.437 nm, an artefact which was confirmed to be caused by self-absorption of the U atomic emission signal [13]. The incorporation of a self-absorption correction term into the spectral-fitting algorithm was found to be inadequate to solve the issue [13].

What we learned from our previous study [13] is that the best approach to correct for self-absorption is by avoiding it. Therefore, the objective of the present study is to identify and test a new set of U emission lines that provide appreciable ^{235}U–^{238}U isotopic shifts and do not suffer from self-absorption for LIBS isotopic analysis in gaseous UF_6 samples. Because LIBS is a fieldable technique requiring no sample preparation, the developed method for direct gaseous UF_6 enrichment assay through calibration solely with theoretical spectral fitting considerably shortens the response time (on-site analysis, with measurement within minutes) of a UF_6 safeguards inspection.

Experimental

With the exception of the optical spectrometer as noted below, the experimental hardware was identical to that previously described [13]. In our previous works [12, 13], a Czerny-Turner grating spectrometer of a focal length of 1.25 m (Horiba Jobin–Yvon 1250 M, Longjumeau, France) was used. Although this spectrometer provides adequate spectral resolution, its physical size (135 × 45 × 37 cm^3) and weight (97 kg) limit its use in the field. For field analysis, the optical spectrometer needs to be of transportable size. As such, a spectrometer with a smaller footprint (DEMON, LTB Lasertechnik Berlin GmbH, Berlin, Germany) was used in the present study. The DEMON spectrometer is of fieldable size (60 × 31 × 23 cm^3) and weight (25 kg). In fact, we placed our DEMON spectrometer on a transportable cart in our laboratory. Albeit only marginally, the DEMON spectrometer offers better spectral resolution than that of the Horiba Jobin–Yvon 1250 M and is adequate for optical isotopic analysis of uranium.

The DEMON is labeled as a Double Echelle Monochromator. Different from the more common Echelle-grating configuration in which the image focal plane is cross dispersed into wavelength and diffraction orders [22–24] (i.e., covering a wide range of wavelengths, often the whole UV–visible), the DEMON uses a prism as a predisperser to first select a small wavelength range to be further dispersed by the Echelle grating. In other words, there is no multiple spectral order overlap in the spectral image after grating dispersion. As such, no cross dispersion after the Echelle grating is needed and an entrance aperture in the form of a slit can be used. This optical arrangement significantly increases light throughput compared to the more common Echelle configuration in which cross dispersion after the grating is needed, because any order sorting after the grating mandates the entrance aperture to be in the form of a small circular or square pinhole, which severely limits the light throughput. Nevertheless, the light throughput of the DEMON spectrometer is less than that of the Horiba Jobin–Yvon 1250 M. Therefore, comparison of LIBS signals reported in the present study with those reported previously [12, 13] need to take into account the light-throughput difference.

For characterization of uranium emission spectra and determination of isotopic shifts, two solid U-glassy samples with natural (i.e., 0.72 atom-%) and highly enriched (~94 atom-%) ^{235}U were measured. These U-glassy samples were prepared through thermal fusion of U_3O_8 and lithium tetraborate at the Y-12 National Security Complex as described in our previous study [12]. The uranium content was approximately 30% by weight [12]. LIBS measurements on U-glassy samples were performed with laser pulse energy of 80 mJ under air at atmospheric pressure. The detector gate delay and width were 8 µs and 25 µs, respectively. A uranium hollow cathode lamp (Glass Expansion, Port Melbourne, Australia) operated under a constant current of 7 mA was used for cross checking of spectral identification.

The UF_6 samples under LIBS measurement are in gaseous form. The UF_6 vapor pressure inside the chamber is indirectly but efficiently varied through the temperature setting of a thermoelectric cooler located underneath the sample chamber. In this work, the UF_6 gas pressure was kept at 15 torr, which corresponded to a temperature of about − 2 °C [25]. All chambers contain UF_6 only, without any buffer gas. The chambers are designed to be gas-tight, chemically compatible with UF_6, and capable to withstand long-duration laser exposure. The detail on the cell design, results of its testing for basic performance, and compatibilities for laser and UF_6 are documented in a separate publication [26]. Unless noted otherwise, the laser pulse energy was 40 mJ.

Journal : Large 10967 | Article No : 8215 | Pages : 13 | MS Code : 8215 | Dispatch : 2-2-2022

Detector gate delay and integrated exposure time for each measurement will be noted in the pertaining discussions. In this paper, all enrichment levels are expressed as atom percent of ^{235}U / ($^{235}U + ^{238}U$). In addition to the two UF_6 samples which contain 0.720% and 4.675% ^{235}U as described in our previous study [13], a third sample containing 9.157% ^{235}U (validated with a multi-collector inductively coupled plasma mass spectrometer at Oak Ridge National Laboratory) also was used in this work.

A nanosecond (~ 5 ns pulse duration, full width at half maximum) Nd:YAG laser operated at its fundamental wavelength at 1064 nm with a repetition rate at 10 Hz was used to generate the LIBS plasma. Plasma emission was collected with a fused-silica lens, sent through an optical fiber, and directed to the DEMON spectrometer equipped with an ICCD detector comprising 1024 × 1024 pixels (DH334T-18F-03, Andor, Belfast, Northern Ireland). The spectrometer was set to a center wavelength of 421.39 nm. The efficiency of an Echelle grating is known to be a strong function of the angle from the grating normal [27], and the spectral response varies greatly [23, 24, 27] even for a small wavelength range within the same grating order. As such, even though the span of the spectral window used in the present study is less than 0.4 nm, spectral-response calibration was necessary and was performed with a NIST traceable UV/VIS deuterium-halogen light source (AvaLight-DH-CAL, Avantes, Broomfield, CO, USA). All presented spectra were corrected for spectral response of the Echelle grating and dark counts of the ICCD detector.

Results and discussion

Spectral window selection and line identification for U enrichment assay

As experimentally shown in our previous study [13], LIBS emission in gaseous UF_6 in the vicinity of 424.4 nm—a wavelength region conventionally and commonly used for optical isotopic analysis of uranium [28–31]—suffers from self-absorption, which consequently leads to a positive bias in the determined ^{235}U assay. Self-absorption is common in LIBS measurements [32–35]. Although different approaches have been reported for compensation of self-absorption, there are multiple sources of uncertainty associated with self-absorption evaluation, in particular for an inhomogeneous plasma [32–35] as in our measurements. Many reported self-absorption compensation methods are good with accuracy only around 10% to 20% [32–34]. In our case, because accurate and precise analytical results better than a few percent are needed for U enrichment assay [36], it is not practical to further investigate and develop a self-absorption compensation subroutine into the spectral-fitting algorithm [13]. Instead, a better approach to handle the self-absorption limitation is by avoiding it.

The ^{238}U II 424.437 nm and its ^{235}U counterpart at 424.412 nm are resonance emission lines [37, 38]. In general, resonance lines suffer from self-absorption more than non-resonance ones. Therefore, the use of non-resonance lines could be a straightforward and viable solution to mitigate the self-absorption limitation. As such, a search for a new spectral window with the following three criteria (in the order of their importance) was conducted. First, no resonance emission lines should be used. Second, the new window should contain multiple, strong U emission lines, in which many, if not all, should possess noticeable isotope shifts. Multiple strong lines avoid the situation in which the isotopic analysis depends primarily on only one line pair. Third, spectral features should be reasonably pure, ideally with no overlapping spectral structure.

Under the right experimental conditions, viz. low UF_6 vapor pressure and low laser pulse energy, the LIBS spectral features from gaseous UF_6 and those from solid U samples are similar [13]. Therefore, it is convenient to use the two atlases published by the Japan Atomic Energy Agency [39, 40] on uranium LIBS spectra for a survey of spectral-window candidates. Several spectral windows with strong and not heavily overlapping U LIBS emission lines were first shortlisted. To down select the candidates, the likelihood of spectral overlap and the lower energy level of the optical transition (i.e., the non-resonance line criterion) were then checked against the high-resolution Fourier transform uranium atlas and spectroscopic database published by the Los Alamos National Laboratory [37]. In the final step of the selection, the isotope shift (IS) of the spectral line contained in each spectral-window candidate was evaluated with reference to the experimental IS-database published by the United Kingdom Atomic Energy Authority [41]. The outcome of this exercise points to a spectral window centered around 421.3 nm to be a good candidate fulfilling the aforementioned three criteria for U isotopic analysis.

Unlike the classical spectral line pair at 424.412–424.437 nm, of which several high-resolution spectra in its wavelength vicinity have been published [28–30], U isotopic analysis with the spectral window at ~ 421.3 nm is unexplored. Therefore, a spectral database needs to be built. First, U emission lines need to be identified. For unambiguous U line identification, three spectra, viz. emission from a U hollow cathode lamp, and LIBS from solid U-glassy sample and gaseous UF_6, were used (Fig. 1a). Because elements other than U are present in these emission sources (e.g., fluorine in UF_6, lithium and boron from lithium borate glass, and neon from the hollow cathode lamp), only those emission lines that are present in all three spectra can be assigned with confidence to be U lines. With the aid from various spectral atlases [37, 38, 41], a total of fourteen U emission lines were

Journal : Large 10967 | Article No : 8215 | Pages : 13 | MS Code : 8215 | Dispatch : 2-2-2022

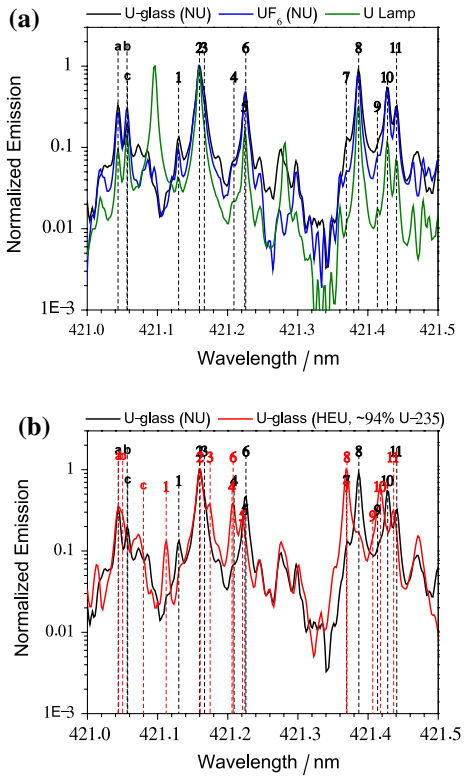

Fig. 1 **a** Identification of ^{238}U emission lines from normalized spectra of three sources: LIBS spectra of a solid U-glassy sample and gaseous UF_6 (with ^{235}U at natural abundance), and emission from a uranium hollow cathode lamp (^{235}U abundance unknown, but likely of natural or depleted). **b** Identification of ^{235}U emission lines and isotopic shifts from LIBS spectra of two solid U-glassy samples with ^{235}U at 0.72% and ~ 94% (HEU, high enriched uranium). The *y*-axis is plotted in logarithmic scale to show the weaker peaks. Intensities are normalized to their respective individual baselines (outside the displayed spectral window). The wavelength positions of the identified spectral peaks for ^{235}U and ^{238}U (see Table 1 for the list) are marked with vertical lines

identified (see Table 1 for assigned wavelength). The identified lines are labeled with two different designations: three in alphabet and eleven in numeric. The three alphabet-labeled lines were found to be not suitable for isotopic analysis; isotopic shift of line *a* is practically zero whereas the ^{238}U component of lines *b* and *c* are practically identical (i.e., direct overlapping). The presence of more than one line with practically identical wavelengths (i.e., direct spectral overlap or line pair with IS ≈ 0) potentially induces redundancy in multivariate nonlinear fitting. As such, only the eleven emission lines labeled with numeric designations are used for U enrichment assay in the multivariate nonlinear spectral model to be discussed in the subsection after next.

Figure 1b shows the normalized LIBS spectra of two solid U-glassy samples, one of which contains ^{235}U at natural abundance and another at a highly enriched level at ~ 94%. The highly enriched sample highlights the isotopic shift (Table 1). Wavelength assignment was performed with a similar procedure as previously described [12]. Although not common, slight adjustments on ^{238}U wavelengths from those values listed in the atlases [37, 38, 41] were needed. For an initial assignment of isotopic shift, the IS tables from Richards and Crew [41] and Smith [42] were used if a particular line can be found therein; otherwise, calculations based on shifts in energy levels as documented in Blaise *et al* [43, 44]. were used. In all cases, the isotopic shifts were then adjusted with reference to the experimental spectrum of the HEU sample presented in Fig. 1b.

In terms of signal-to-background ratios, the U spectral lines in the spectral window centered at 421.3 nm are comparable to the classical line for U isotopic analysis at 424.437 nm. Figure 2 shows the measured spectra from 421.10 nm to 421.46 nm of two gaseous UF_6 samples with ^{235}U at 0.720% (i.e., NU) and 4.675% (i.e., low enriched uranium, LEU). The ^{235}U–^{238}U isotopic shifts are distinctly identifiable between the LEU and the NU samples (see Peaks #8 and #10 in Fig. 2, for example). The spectra are normalized to their individual baselines with an assigned value of 1. The peak intensities of multiple, strong U lines are in the range of 3 to 5 under this normalized scale, which means that the signal-to-background ratios are between 2 and 4. Under identical conditions of 15 torr UF_6 and 40 mJ laser pulse energy, the reported signal-to-background ratio of the U 424.437 nm line was ~ 3.5 [13].

Evaluation of self-absorption of U lines in the spectral window centered at 421.3 nm

Before further discussion on the development of our spectral-fitting algorithm for this new spectral window centered at 421.3 nm, it is crucial to assess any extent of self-absorption of U lines in this window. After all, theory predicts that the use of non-resonance emission lines only reduces the likelihood, but does not guarantee the absence of self-absorption [35, 45]. In our previous work [13] using the classic spectral window centered at 424.4 nm, a large positive bias was observed in the determined ^{235}U abundance for a LEU sample (with reference ^{235}U content at 4.675%), and the bias increased monotonically with laser pulse energy (see Fig. 3). Through confirmation with an independent experiment previously reported [13], the increasing bias of the determined ^{235}U content with applied laser pulse energy is a result of self-absorption. In brief, self-absorption is proportional to the number densities of the absorbing species (the ^{235}U and ^{238}U free atoms or atomic ions in this specific case) and higher laser pulse energy creates more uranium atoms and atomic ions. For a UF_6 sample with ~ 4.7% enrichment, the number density of ^{238}U is roughly 20 × that of ^{235}U. Accordingly, self-absorption for ^{238}U is more severe than that for ^{235}U, and hence, ^{238}U emission is absorbed to

Journal : Large 10967 | Article No : 8215 | Pages : 13 | MS Code : 8215 | Dispatch : 2-2-2022

Table 1 List of ^{235}U and ^{238}U emission lines, their associated weighting factor (α), and isotopic shift (IS = $\lambda^{\circ}_{235} - \lambda^{\circ}_{238}$) for spectral fitting

Line number, i	α	$\lambda^{\circ}_{238,\,i}$ (nm)	$\lambda^{\circ}_{235,\,i}$ (nm)	IS (pm)	Line Assignment* [38] (Lower – Upper, with energy levels given in unit of cm^{-1})	Remarks (λ°_{238} and IS are listed in units of nm and pm, respectively)
a	–	421.0438	421.0442	0.4	U II $^{6}L^{\circ}_{6.5} - {}^{0}A_{5.5}$ (1,749.12–25,492.92)	λ = 421.0440 [37], 421.045 [41] IS = + 1 [41], + 1.1 [44]
b	–	421.0567	421.0502	–6.5	U I $^{5}K^{\circ}_{7} - {}^{0}A_{7}$ (7,326.12–31,069.20)	λ = 421.0568 [37] IS = –6.0 [43]
c	–	421.0574	421.0798	22.4	Unknown	λ = 421.058 [41] IS = + 13 [41]
1	k	421.1302	421.1122	–18.0	U II $^{4}I^{\circ}_{5.5} - {}^{0}A_{6.5}$ (4,420.87–28,159.82)	λ = 421.130 [41] IS = –16 [41]
2	1/k	421.1599	421.1607	0.8	U I $^{7}M^{\circ}_{6} - {}^{0}A_{6}$ (6,249.03–29,986.32)	λ = 421.1594 [37], 421.160 [41] IS = + 1 [41], + 1.2 [43]
3	1	421.1669	421.1748	7.9	U II $^{6}M^{\circ}_{6.5} - {}^{0}A_{5.5}$ (4,585.43–28,322.36)	λ = 421.1658 [37], 421.166 [41], 421.16 [42] IS = + 10 [41], + 7 [42]
4	1/k	421.2091	421.2061	–3.0	U II $^{4}I_{5.5} - {}^{0}A^{\circ}_{4.5}$ (11,389.47–35,124.03)	λ = 421.209 [41] IS = 0 [41]
5	1/k	421.2245	421.2211	–3.4	U I $^{7}M^{\circ}_{8} - {}^{0}A_{9}$ (10,347.34–34,080.96)	λ = 421.2247 [37] IS = –4.5 [43]
6	k	421.2259	421.2078	–18.1	U II $^{4}I^{\circ}_{5.5} - {}^{4}K_{5.5}$ (4,420.87–28,154.45)	λ = 421.226 [41], 421.23 [42] IS = –16 [41], –18 [42], –17.4 [44]
7	1/k	421.3693	421.3693	0.0	U II $^{4}K^{\circ}_{7.5} - {}^{0}A_{6.5}$ (13,015.84–36,741.20)	λ = 421.370 [41] IS = 0 [41]
8	k	421.3868	421.3699	–16.9	U I $^{5}L^{\circ}_{9} - {}^{7}N_{10}$ (11,308.15–35,032.66)	λ = 421.3864 [37], 421.387 [41], 421.39 [42] IS = –17 [41], –20 [42], –16.9 [43]
9	1	421.4136	421.4067	–6.9	U I $^{3}H^{\circ}_{5} - {}^{0}A_{5}$ (10,255.00–33,977.98)	λ = 421.4134 [38] IS = –4.1 [43]
10	k	421.4280	421.4176	–10.4	U I $^{3}I^{\circ}_{5} - {}^{0}A_{5}$ (5,762.08–29,484.19)	λ = 421.4275 [37], 421.428 [41] IS = –9 [41], –5.0 [43]
11	1/k	421.4409	421.4365	–4.4	U II $^{6}L^{\circ}_{5.5} - {}^{0}A_{5.5}$ (289.04–24,010.47)	λ = 421.4411 [37], 421.441 [41] IS = –4 [41], –4.3 [44]

*Line with unknown spin multiplicity or total orbital quantum number (*L*) are listed as 0 and A, respectively, in its spectroscopic term symbol

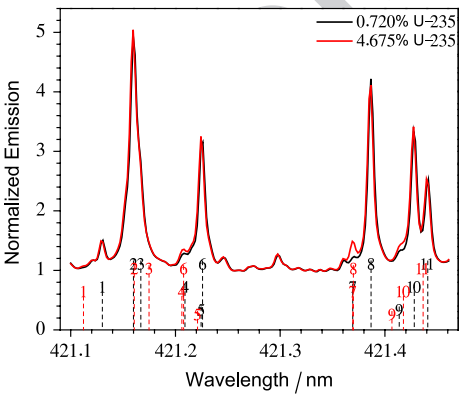

Fig. 2 Measured LIBS emission spectra from two UF_6 samples (with 0.720% and 4.675% ^{235}U), showing the appreciable isotopic peaks from ^{235}U. Spectra were taken with UF_6 at a pressure of 15 torr and with laser pulse energy of 40 mJ. The wavelength positions of the identified spectral peaks for ^{235}U and ^{238}U (see Table 1 for the list) are marked with vertical lines

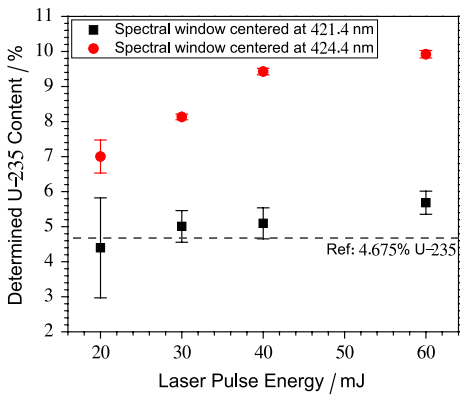

Fig. 3 Determined ^{235}U content of a LEU UF_6 sample (^{235}U reference value = 4.675%) with the optimized, nonlinear spectral-fitting algorithm as a function of laser pulse energy for two spectral windows – the classic one centered at 424.4 nm (data from our previous study [13]) and the new one from the present study centered at 421.4 nm. In all cases, the UF_6 pressure was 15 torr. The error bar represents the standard deviation of three replicate measurements, each with signal accumulation from 1200 laser pulses

Journal : Large 10967 | Article No : 8215 | Pages : 13 | MS Code : 8215 | Dispatch : 2-2-2022

a greater extent. Because of the more attenuated ^{238}U counterpart, the ^{235}U peak on a relative scale appears stronger than it should be, which then leads to a positive bias in the determined ^{235}U content.

To assess self-absorption in this new spectral window, an enrichment assay of the same LEU UF_6 sample was studied as a function of laser pulse energy. A multivariate nonlinear spectral fitting, to be discussed in detail in the next section, was applied to the measured spectra to determine the ^{235}U content. As shown in Fig. 3, except for the highest studied laser pulse energy of 60 mJ, the determined $[^{235}U / (^{235}U + ^{238}U)]$ ratios appear flat and agree with the reference value within experimental uncertainties, an observation indicating the absence of appreciable self-absorption for U emission lines in this new spectral window.

Development of spectral-fitting algorithm

Similar to our previous work [12, 13], extraction of U isotopic information from the measured spectra is through multivariate nonlinear spectral fitting, which is theoretical in basis and does not require calibration with isotopically enriched standards. In addition to setting up a new spectral database (see Table 1), further development of the fitting algorithm is needed because many weak, not readily identifiable spectral peaks are present in the spectral window (see Fig. 1b). Furthermore, each spectral line pair should not (and does not) contribute the same weight to the enrichment assay. More details on these two points and a proposed solution will be discussed in detail in subsequent sub-sections.

The development of the fitting algorithm is guided by the root mean square error (RMSE) of a set of UF_6 samples comprising three enrichment levels – 0.720%, 4.675% and 9.157%. A set of twelve spectra, each with accumulated LIBS emission from 3000 laser pulses at 10 Hz (i.e., 5 min) was measured for each UF_6 sample. As will be discussed, because one parameter in the fitting model (k in Table 1, which is a weighting factor based on the relative magnitude of isotopic shift and will be discussed in detail in subsequent discussion) was optimized through an empirical approach, it is important to verify that the optimized value of this parameter is generally applicable to other spectra taken under similar conditions. To elaborate, overfitting occurs when a modeling function follows too closely to the training data set, including the specific noise therein [46, 47]. Consequently, overfitting gives very low error in the training data set, but the results are not generalizable to fit additional unseen data. As such, the best practice to avoid overfitting is to verify the model with an independent data set (typically referred to as testing or verification data set) [46, 47]. Furthermore, because slight drifts in day-to-day operation or different measurements are possible, we acquired a separate set of spectra for validation with an intentional shift of the detector delay time by 0.1 µs to mimic the effect of slight drift in the operation and to make sure that the training and validation data sets are not identical. For ease of discussion, the spectra set which forms the basis for the determination of the empirical parameter k in the fitting model (i.e., the training data) is referred to as Data Set A, whereas those taken for verification with a 0.1-µs shift in delay time (i.e., the validation data) is referred to as Data Set B.

The root mean square error (RMSE) is defined as

$$RMSE = \sqrt{\frac{\sum_{k=1}^{n} \left(R_{det,k} - R_{ref,k}\right)^2}{n}} \quad (1)$$

where $R_{det,k}$ and $R_{ref,k}$ are, respectively, the determined and reference U isotopic ratios of the k^{th} sample, and n is the total number of samples. From its definition, the RMSE reflects both the accuracy and precision of a method if replicated measurements of a sample are presented individually to the calculation of RMSE. Because analytical accuracy is of prime importance in the development of fitting algorithm, the twelve collected spectra from each sample were averaged before spectral fitting.

In this work, all algorithms are of multiple line-pair spectral fitting as previously described [12] and takes the general form (Eq. 2):

$$I^{expt}(\lambda) = \sum_{\forall i} \left\{ \frac{RH_i\omega^2}{\left[4\left(\lambda - \lambda_s - \lambda^{o}_{235,i}\right)^2 + \omega^2\right]} + \frac{(1-R)H_i\omega^2}{\left[4\left(\lambda - \lambda_s - \lambda^{o}_{238,i}\right)^2 + \omega^2\right]} \right\} + c_0 + \varepsilon(\lambda) \quad (2)$$

The first and second terms inside the summation bracket represent the spectral profiles from ^{235} and ^{238}U, respectively. $I^{expt}(\lambda)$ is the experimental spectrum; λ and λ_s are respectively the measured wavelength and a correction factor for wavelength shifts between wavelength calibration and measurement; λ^{o} denotes the center wavelength of the atomic emission line; H is the spectral-peak height; ω is the linewidth, which is assumed to be identical for all emission lines; c_0 represents the plasma continuum background, which is assumed to be a constant in this small wavelength range;

R is the [^{235}U / (^{235}U + ^{238}U)] ratio; and $\varepsilon(\lambda)$ is the fitting residual. In this work, eleven spectral lines are fitted to the measured spectrum, and variables denoted with a subscript i refer to spectral-line specific parameters (see Table 1). The fitting algorithm utilizes the Levenberg–Marquardt method to locate the optimal combination of the variables for the minimization of the sum of the residual square (S^2). As will be discussed in subsequent sub-sections, for some tested fitting algorithms, wavelength-dependent weighting factors, wt(λ), are applied to different data points in the acquired spectrum. S^2 takes the general form:

$$S^2 = \sum \mathrm{wt}(\lambda) \times [\varepsilon(\lambda)]^2 \quad (3)$$

Direct, no-weight spectral fitting

In direct, no-weight spectral fitting, the acquired spectrum between 421.099 nm and 421.460 nm is fitted for the eleven U emission line pairs (see Table 1) with wt(λ) = 1 for all data points in the spectrum. As shown in Table 2, the results are unsatisfactory. The fitting algorithm was unable to extract the ^{235}U component in the spectrum of the NU sample and returned 0% ^{235}U. The ^{235}U contents of the two LEU samples also were underestimated by more than 2% in absolute scale. The RMSE of the three UF_6 samples, obtained with two slightly different measurement conditions, was large and was close to 2.5% in absolute ^{235}U content.

The unsatisfactory results of the direct, no-weight fitting method is likely a consequence of the presence of "outliers" in the measured spectrum. In this context, outlier is any spectral feature not included in the fitting model, for example, measurement noise or spectral peaks not belonging to the eleven spectral line pairs in the fitting model (Table 1). It is well known that the convergence or quality of least-square fitting is often compromised by the presence of only a small number of ill-fit data points or outliers [48, 49]. Because the database for spectral fitting (Table 1) is incomplete, abundant outliers not accountable by the fitting model are present in this case (see Fig. 1a). A possible solution to reduce the impact of outliers to the sum of residual square (S^2) is with tailored weighing factor (Eq. 3).

Iterative spectral fitting with wavelength-dependent weighting factor corresponding to spectral line position in the fitting database

For the next developed algorithm, the fitting is forced to focus only on the spectral regions in which ^{235}U and ^{238}U emission line pairs are defined (i.e., Table 1). Because many fitted spectral profiles from gaseous UF_6 samples gave a half width between 0.007 nm to 0.008 nm, simulated peak shapes with a Lorentzian spectral profile and half width of 0.0075 nm were used directly as the wavelength-dependent weighting factor. All listed ^{235}U and ^{238}U spectral lines contribute equally to the weighting factor. As such, wt(λ) takes the form:

$$\mathrm{wt}(\lambda) = \sum_{\forall i} \left\{ \frac{0.0075^2}{\left[4\left(\lambda - \lambda^{o}_{235,i}\right)^2 + 0.0075^2\right]} + \frac{0.0075^2}{\left[4\left(\lambda - \lambda^{o}_{238,i}\right)^2 + 0.0075^2\right]} \right\} \quad (4)$$

where λ and λ^o denotes respectively the measured wavelength and the center wavelength of the emission line in the fitting database (Table 1), with all wavelengths expressed in nm units. Because of the presence of wavelength shifts between wavelength calibration and measurement (i.e., λ_s in

Table 2 Determined [^{235}U / (^{235}U + ^{238}U)] ratios of the three tested UF_6 samples with the four candidate algorithms, which incorporate increasing number of factors into the fitting weight

Data set	A (ICCD delay = 4.0 μs)			B (ICCD delay = 3.9 μs)			RMSE (Set A & B)
Sample	NU	LEU #1	LEU #2	NU	LEU #1	LEU #2	
Reference ^{235}U abundance	0.720%	4.675%	9.157%	0.720%	4.675%	9.157%	
I – Direct, no-weight spectral fitting	0%	1.028%	7.138%	0%	1.045%	6.776%	2.492%
II – Iterative spectral fitting; simulated spectral line profiles as λ-dependent weighting factor; equal weights for ^{235}U and ^{238}U components; no line-dependent weighting factor (i.e., $\alpha = k = 1$)	0%	2.438%	7.786%	0%	2.472%	7.538%	1.602%
III – Similar to II, except that fitting weight for ^{235}U and ^{238}U components is inversely proportional to the determined isotopic ratio	0%	3.342%	8.145%	0%	3.375%	7.964%	1.076%
IV – Similar to III, except that inclusion of isotopic shift-based weighting factor α, with $k = 2.25$, is applied to emission line (see Table 1)	0.251%	5.058%	9.384%	0.337%	5.100%	9.206%	0.353%

Twelve spectra, each with accumulated LIBS signals from 3000 laser shots, were averaged before presented for spectral fitting

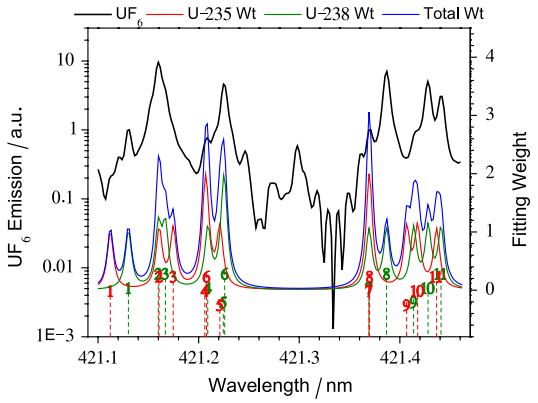

Fig. 4 Measured LIBS emission spectrum from a LEU UF_6 sample with ^{235}U reference value of 4.675%, and the associated wavelength-dependent weighting factor incorporated with only spectral line positions (see text for discussion). The wavelength positions of the ^{235}U and ^{238}U spectral peaks are marked with vertical lines

Eq. 2), an iterative approach is used. The calibrated wavelength is corrected for wavelength shift through the value of determined λ_s from the previous iteration. The array of wavelength-dependent weighting factors is then recalculated with the re-calibrated wavelength, and the fitting is performed again until the determined U isotopic ratio of the sample, R, converges.

Figure 4 shows the measured spectrum from the 4.675% LEU UF_6 sample and the associated weighting factor of the described approach. Measured spectral peaks not identified in the fitting database are assigned with low weighting factors, close to zero in many cases. The most distinct example is the weighting factor of practically zero (and hence negligible contribution to S^2) for the spectral peaks between 421.26 nm and 421.34 nm. Compared to the no-weight direct fitting approach, although the RMSE was improved to 1.6% ^{235}U (see Table 2), results remain unsatisfactory. Specifically, the algorithm was still unable to determine the ^{235}U component in the NU sample and returned 0% ^{235}U abundance.

It should be noted that the simple wavelength-dependent weighting factor, based on spectral peaks contained in the fitting database, compensates the effect of measured spectral peaks (as outliers) that are not present in the fitting model, but does not correct for other factors that are known to contribute to bias in least-square regression. One pre-requisite for the success of least-square regression is that experimental uncertainties are statistically identical for all the data points (i.e., the homoscedasticity requirement) [48, 50–54], a condition which is not fulfilled in our measurements. Taking the NU UF_6 sample as an example, the ^{235}U component is ~ 138 × weaker than that of the ^{238}U counterpart. As such, the absolute noise level (both source flicker and shot noise) in the ^{238}U component is larger. During the search for the best combination of fitting variables and particularly in the presence of measurement noise, the contribution of the small ^{235}U spectral features could be completely ignored by the algorithm if fitting only to the much large ^{238}U peaks provides a global minimization of S^2. This known limitation of least-square fitting, once again, can be corrected by the use of tailored weighting factor [48, 50–54].

Inclusion of determined isotopic ratio into weighting factor for iterative spectral fitting

The general approach to correct for the uneven uncertainty distribution (i.e., heteroscedasticity) in data points is to set a weighting factor *inversely* proportional to the variance (σ^2) of the data point [48, 50, 51]. However, a slightly different approach is used here. For photon shot-noise limited uncertainty, the ratio of the variance of the two isotopic spectral peaks is directly proportional to their emission intensities, which in turn is directly proportional to their respective isotopic contents in the sample. Accordingly, the weighting factors for the ^{235}U and ^{238}U lines are no longer set to be identical but inversely proportional to their isotopic abundance as determined in the previous iteration. For instance, if the determined isotopic abundance of ^{235}U:^{238}U is 2:98, the weighting factor is set to 98:2 for the ^{235}U–^{238}U line pair in the next iteration. A limiting factor is needed if the previous iteration returns 0% of one isotope. In this case, a lower limit of 0.05% is set for the isotope with zero abundance. In other words, the maximum ratio of the weighting factor between the two isotopes is 1999. In the first iteration, a 50–50 abundance ratio is assumed for ^{235}U and ^{238}U (i.e., equal weighing). The set of newly determined ^{235}U and ^{238}U isotopic abundance after each iteration is then used to set the weighing factor for the next iteration. In the present approach, wt(λ) takes the form:

$$\mathrm{wt}(\lambda) = \sum_{\forall i} \left\{ \frac{0.0075^2}{R\left[4\left(\lambda - \lambda^{o}_{235,i}\right)^2 + 0.0075^2\right]} + \frac{0.0075^2}{(1-R)\left[4\left(\lambda - \lambda^{o}_{238,i}\right)^2 + 0.0075^2\right]} \right\} \quad (5)$$

Journal : Large 10967 | Article No : 8215 | Pages : 13 | MS Code : 8215 | Dispatch : 2-2-2022

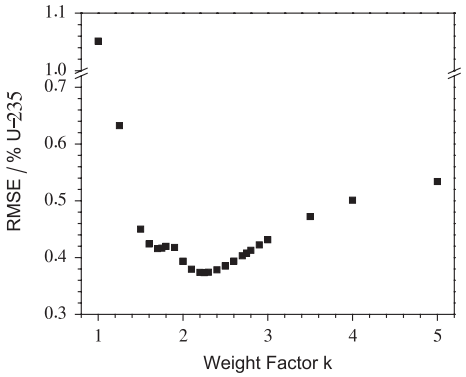

Fig. 5 RMSE of three UF_6 samples (Data Set A, with detector delay time of 4.0 μs) as a function of k – the isotopic shift-based weighting factor

The effectiveness of inclusion of the determined isotopic ratio into the weighting factor is demonstrated by the further improvement of RMSE from 1.60% to 1.08% of ^{235}U (see Table 2). Although the determined ^{235}U contents were closer to their respective reference values for the two LEU UF_6 samples, the fitting algorithm still returned 0% ^{235}U for the NU UF_6 sample.

Weighting factor based on isotopic shift of the line pair

Up to this point, all emission line pairs listed in the spectral fitting database (Table 1) carry equal weight. However, their isotopic shifts vary from < 1 pm to 18 pm. For emission lines whose isotopic shifts are significantly larger than the measured line width (typical ~ 7.5 pm), the shifts are visually distinct, and extraction of isotopic information should be comparatively unambiguous. In contrast, isotopic analysis would become more difficult and less reliable when the isotopic shifts are only a fraction of the measured line width. Therefore, it is reasonable to include another weighting factor that reflects the isotopic shift. This isotopic shift-based weighting factor is emission line specific and is termed α in Table 1. The measured line width of 7.5 pm is used as a reference and lines with isotopic shifts larger than 10 pm are assigned a weight factor that are k times larger than lines having shift around 7.5 pm. Likewise, the weighting factor is reduced and α is assigned as $1/k$ for lines with shift that are less than 5 pm. Depending on the isotopic shift, k (> 1) appears as an emphasizing (as multiplication) or an attenuating (as division) weighting factor for a candidate line pair (Table 1). The isotopic shift-based weighting factor, wt(λ), takes the form:

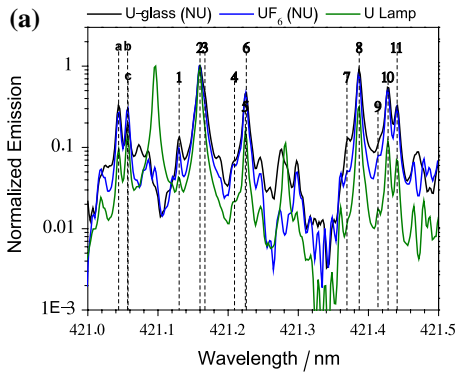

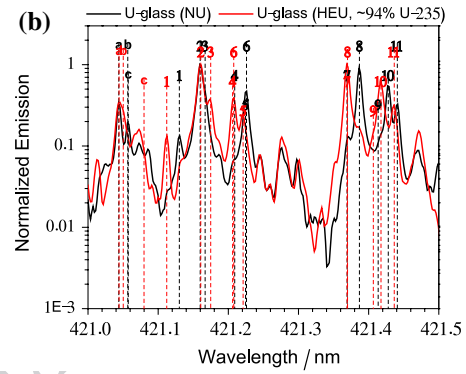

Fig. 6 **a** Measured LIBS emission spectrum from a LEU UF_6 sample with ^{235}U reference value of 4.675%, and the associated wavelength-dependent weighting factor incorporated with (i) spectral line positions, (ii) determined isotopic ratio, and (iii) isotopic shifts (see text for discussion). The wavelength positions of the ^{235}U and ^{238}U spectral peaks are marked with vertical lines. **b** The measured and fitted emission spectra, and the fitting residual

Figure 5 shows the effect of the isotopic shift-based weighting factor k on the RMSE of the enrichment assay of the three UF_6 samples. It should be noted that the RMSE in Fig. 5 was evaluated only with Data Set A (i.e., 4.0 μs delay). The use of only one data set is intentional as such an arrangement allows us to evaluate if the determined optimal value of k can be readily transferred to other measurements under similar, but not identical, experimental conditions (e.g., Data Set B). The inclusion of weighting factor k improves RMSE. For instance, without the use of this isotopic shift-based weighting factor (i.e., $k = 1$), the RMSE of Data Set A was 1.05 and quickly reduced to 0.63 for a small k of 1.25. The RMSE kept improving until k reached about 2.25 for a lowest RMSE value of 0.37. Thereafter, RMSE gradually increased (Fig. 5). With the 4.675% ^{235}U LEU UF_6 sample as an example, Fig. 6a shows the measured spectrum

$$\mathrm{wt}(\lambda) = \sum_{\forall i} \left\{ \frac{\alpha_i 0.0075^2}{R\left[4\left(\lambda - \lambda^{o}_{235,i}\right)^2 + 0.0075^2\right]} + \frac{\alpha_i 0.0075^2}{(1-R)\left[4\left(\lambda - \lambda^{o}_{238,i}\right)^2 + 0.0075^2\right]} \right\} \quad (6)$$

and the total fitting weights including all discussed factors whereas Fig. 6b depicts the fitting quality and residual.

Table 2 lists the determined ^{235}U contents of the three UF_6 samples measured under two experimental conditions differing by a delay time of 0.1 μs, with *k* set at 2.25. The optimal value of 2.25 for *k*, determined with Data Set A, is also applicable to Data Set B. In fact, the overall analysis results, as reflected by the differences between the determined and the reference ^{235}U contents in the three samples, were marginally better for Data Set B. The overall RMSE was 0.35% ^{235}U. The algorithm returned non-zero ^{235}U content for the NU UF_6 sample. An independent analysis with Data Set B also revealed that the optimal *k* value was 2.25.

Analytical accuracy and precision of the optimized spectral-fitting algorithm

From the foregoing discussion, weighted spectral fitting incorporating factors like (i) spectral line positions, (ii) determined isotopic ratio, and (iii) isotopic shift, are essential for correct extraction of isotopic information from LIBS spectra of gaseous UF_6. To evaluate the accuracy and precision of the spectral-fitting approach for UF_6 enrichment assay, individual measured spectra (each with LIBS signals accumulated from 3000 laser shots, and twelve spectra for each sample) were presented for isotopic analysis. To further assess the effect of a slight shift in measurement conditions, the delay time of one set of measurement was intentionally lengthened from 4.00 μs to 4.14 μs (Data Set C). It also should be mentioned that Data Set C was taken months apart from that of Data Set A and B, so that the medium-term reproducibility of the method also could be estimated.

Table 3 lists the twelve replicates of the different measurements, together with their statistics. For the two LEU samples, the RSDs were in the range of 2% to 5%; RSD for the NU sample was much larger because of the small value of ^{235}U in the denominator of the RSD calculation. Overall, the standard deviation of the measurements, in terms of *absolute* ^{235}U content, appeared independent of the ^{235}U content and typically ranged between 0.2% and 0.5%. Likewise, although one measurement (the 4.675% LEU sample in Data Set C) gave an absolute bias of 0.83% ^{235}U, other measurement biases were contained within ± 0.5% in *absolute* ^{235}U (Table 3).

The achievable accuracy and precision of UF_6 enrichment assay with laser induced plasma and theoretical spectral fitting compare favorably with other fieldable, optical-based techniques, namely, high performance infrared (HPIR) spectroscopy [6, 7] and atomic beam laser absorption spectroscopy [10, 11]. For example, UF_6

Table 3 Determined [^{235}U / (^{235}U + ^{238}U)] ratios of the three tested UF_6 samples with the developed multivariate nonlinear spectral fitting algorithm

Replicate	A (ICCD delay = 4.0 μs)			B (ICCD delay = 3.9 μs)			C (ICCD delay = 4.14 μs)		
	NU (%)	LEU #1 (%)	LEU #2 (%)	NU (%)	LEU #1 (%)	LEU #2 (%)	NU (%)	LEU #1 (%)	LEU #2 (%)
1	0.05	5.00	9.07	0.35	5.13	9.28	0.39	5.59	8.73
2	0.35	5.06	9.18	0.21	5.02	9.22	0.75	5.46	9.07
3	0	4.92	9.48	0.58	4.96	8.89	0.78	5.40	9.07
4	0.48	5.17	9.30	0.25	4.98	9.13	0.88	5.45	9.17
5	0.17	4.89	9.33	0.22	5.16	9.30	0.83	5.45	8.70
6	0.30	4.98	9.01	0.41	5.36	9.50	0.85	5.57	8.73
7	0.17	5.01	9.27	0.15	5.07	8.92	1.01	5.9	9.14
8	0.34	4.84	9.88	0.29	5.12	9.47	1.15	5.52	9.80
9	0.06	5.10	9.51	0.30	5.17	9.37	0.86	5.51	8.80
10	0.38	5.35	9.25	0.29	4.94	8.99	0.49	5.34	9.65
11	0.41	5.13	9.45	0.50	5.24	9.21	0.93	5.75	10.08
12	0.37	5.29	9.83	0.68	5.07	9.25	1.14	5.74	9.73
Average	0.26	5.06	9.38	0.35	5.10	9.21	0.84	5.51	9.22
SD	0.16	0.16	0.27	0.16	0.12	0.20	0.23	0.14	0.48
RSD	63	3.1	2.9	46	2.4	2.1	27	2.6	5.2
Reference ^{235}U	0.720	4.675	9.157	0.720	4.675	9.157	0.720	4.675	9.157
Bias (absolute)	–0.46	0.39	0.22	–0.37	0.43	0.05	0.12%	0.83	0.07
Bias (relative)	–64	8.3	2.4	–51	9.1	0.58	16	18	0.72

Fitting weight include contributions from simulated spectral profile, determined ^{235}U abundance, and an isotopic shift-based weighting factor (α, with *k* = 2.25). Twelve spectra, each with accumulated LIBS signals from 3000 laser shots, were measured for each sample

Journal : Large 10967 | Article No : 8215 | Pages : 13 | MS Code : 8215 | Dispatch : 2-2-2022

samples ranging from depleted to highly enriched ^{235}U levels were analyzed with the HPIR method, and the reported standard deviations of the measurements showed no correlation with the ^{235}U content and ranged between 0.14% and 0.52% of *absolute* ^{235}U [6, 7]. In atomic beam laser absorption spectroscopy, measurement uncertainties between 0.2% and 0.3% in *absolute* ^{235}U content were reported [10, 11].

Conclusion

A new spectral window, centered at around 421.3 nm, was found to be suitable for direct gaseous UF_6 enrichment assay using LIBS. No appreciable self-absorption was observed for U emission lines in this spectral window, in marked contrast to the spectral window containing the classical U II 424.437 nm line. An iterative, multivariate nonlinear spectral fitting algorithm, which can extract enrichment information directly from the measured LIBS spectra was developed and evaluated. Because this spectral window contains numerous spectral lines with non-negligible emission, it is not practical to have the wavelength of each of them well characterized, and weighting factors for spectral fitting were found to be necessary. Wavelength-dependent weighting factors, which take into consideration the spectral positions, determined isotopic ratio, and isotopic shift of the emission line pairs, is applied in an iterative fashion. Overall, the speed of the iterative spectral fitting is fast and acceptable for in-field analysis. In this work, all fittings were performed on an older laptop computer (CPU: Intel Core i7-3630QM) with a custom programming script written in OriginLab software. It often took less than 90 s for fitting a single spectrum, although some spectra took longer (up to 300 s) for convergence. Although the developed spectral-fitting algorithm does not require the use of calibration standards, it does not preclude the use of isotopically enriched standards for calibration for further improvement in the analytical accuracy. For instance, a hydride calibration model, in which either the spectral fitting-determined isotopic ratio is re-calibrated with the reference values of a set of calibration standards or a correction factor could be applied to fine-tune the determined isotopic ratio, can be envisioned.

The development of direct UF_6 enrichment assay with LIBS offers unique analytical capability. Its no-sample-preparation approach, short measurement and data processing times (minutes), together with instrument hardware footprint similar to a small shopping cart, make it a suitable candidate for UF_6 enrichment assay in the field. In addition, because both the ^{235}U and ^{238}U spectral lines are measured simultaneously, the flicker noise associated with pulse-to-pulse fluctuation of the laser can be effectively cancelled through ratioing. Further development for measurement and testing in a simulated field environment are underway.

Acknowledgements This work was supported by the National Nuclear Security Administration's Defense Nuclear Nonproliferation Office of Research and Development of the U.S. Department of Energy under contract numbers DE-AC02-05CH11231 at the Lawrence Berkeley National Laboratory and DE-AC05-00OR22725 at the Oak Ridge National Laboratory.

References

1. Meija J, Coplen TB, Berglund M, Brand WA, Bièvre PD, Gröning M, Holden NE, Irrgeher J, Loss RD, Walczyk T, Prohaska T (2016) Isotopic compositions of the elements 2013 (IUPAC technical report). Pure Appl Chem 88:293–306
2. Morse EC (2016) The nuclear fuel cycle. Analytical methods for nonproliferation. Springer, Cham, Switzerland, pp 71–92
3. Kessler G (2012) Uranium enrichment. Sustainable and safe nuclear fission energy: technology and safety of fast and thermal nuclear reactors. Springer, Berlin, Germany, pp 59–71
4. Groult H, Lantelme F, Salanne M, Simon C, Belhomme C, Morel B, Nicolas F (2007) Role of elemental fluorine in nuclear field. J Fluorine Chem 128:285–295
5. Chan GCY, Valentine JD, Russo RE (2017) Towards novel field-deployable instrumentation for UF_6 enrichment assay – an overview of existing and emerging technologies. ESARDA Bull 54:31–43
6. Strange Fessler KA, O'Rourke P, DeRoller N, Simmons D, Serkiz S (2020) Infrared spectroscopic method for uranium isotopic analysis. Proc SPIE 11416, Chemical, Biological, Radiological, Nuclear, and Explosives (CBRNE) Sensing XXI 11416:114160R
7. Fessler KAS, O'Rourke PE, DeRoller NF, Simmons D, Serkiz SM (2021) Use of an infrared spectroscopic method for isotopic analysis of gaseous uranium hexafluoride. In: Srivatsan TS, Harrigan WC, Hunyadi Murph S (eds) Metal-matrix composites – advances in analysis, measurement, and observations. Springer, Cham, Switzerland, pp 183–199
8. Nabiev SS, Semenov VM, Stavrovskii DB, Men'shikov PL, Men'shikov LI, Grigor'ev GY (2017) Measurements of the isotopic composition of UF_6 according to the fine structure of the IR absorption spectrum in the v1 + v3 band. Russ J Phys Chem B 11:61–76
9. Golubkov GV, Grigoriev GY, Nabiev SS, Palkina LA, Golubkov MG (2018) Use of IR absorption laser spectroscopy at nuclear fuel cycle plants: problems and prospects (review). Russ J Phys Chem B 12:804–829
10. Lebedev V, Bartlett JH, Castro A (2018) Isotope-resolved atomic beam laser spectroscopy of natural uranium. J Anal At Spectrom 33:1862–1866
11. Bartlett JH, Castro A (2019) Isotopic spectroscopy of uranium atomic beams produced by thermal reduction of uranium compounds. Spectrochim Acta Part B 155:61–66
12. Song J, Chan GCY, Mao X, Woodward JD, Smithwick RW, Schaaff TG, Stowe AC, Harris CD, Zheng R, Zorba V, Russo RE (2018) Multivariate nonlinear spectral fitting for uranium isotopic analysis with laser-induced breakdown spectroscopy. Spectrochim Acta Part B 150:67–76
13. Chan GCY, Martin LR, Trowbridge LD, Zhu ZL, Mao XL, Russo RE (2021) Analytical characterization of laser induced

plasmas towards uranium isotopic analysis in gaseous uranium hexafluoride. Spectrochim Acta Part B 176:106036
14. Quentmeier A, Bolshov M, Niemax K (2001) Measurement of uranium isotope ratios in solid samples using laser ablation and diode laser-atomic absorption spectrometry. Spectrochim Acta Part B 56:45–55
15. Bushaw BA, Anheier NC Jr (2009) Isotope ratio analysis on micron-sized particles in complex matrices by laser ablation-absorption ratio spectrometry. Spectrochim Acta Part B 64:1259–1265
16. Miyabe M, Oba M, Iimura H, Akaoka K, Maruyama Y, Ohba H, Tampo M, Wakaida I (2013) Laser ablation absorption spectroscopy for remote analysis of uranium. Hyperfine Interact 216:71–77
17. Lebedev V, Bartlett JH, Malyzhenkov A, Castro A (2017) Microchannel array crucible for isotope-resolved laser spectroscopy of high-temperature atomic beams. Rev Sci Instrum 88:126101
18. Senesi GS, Harmon RS, Hark RR (2021) Field-portable and handheld laser-induced breakdown spectroscopy: historical review, current status and future prospects. Spectrochim Acta Part B 175:106013
19. Rakovský J, Čermák P, Musset O, Veis P (2014) A review of the development of portable laser induced breakdown spectroscopy and its applications. Spectrochim Acta Part B 101:269–287
20. Harilal SS, Brumfield BE, LaHaye NL, Hartig KC, Phillips MC (2018) Optical spectroscopy of laser-produced plasmas for standoff isotopic analysis. Appl Phys Rev 5:021301
21. Wu J, Qiu Y, Li X, Yu H, Zhang Z, Qiu A (2020) Progress of laser-induced breakdown spectroscopy in nuclear industry applications. J Phys D: Appl Phys 53:023001
22. Becker-Ross H, Florek SV (1997) Echelle spectrometers and charge-coupled devices. Spectrochim Acta Part B 52:1367–1375
23. Bibinov N, Halfmann H, Awakowicz P, Wiesemann K (2007) Relative and absolute intensity calibrations of a modern broadband echelle spectrometer. Meas Sci Technol 18:1327–1337
24. Taleb A, Shen C, Mory D, Cieślik K, Merk S, Aziz MR, Caricato AP, Gerhard C, Pelascini F, Hermann J (2021) Echelle spectrometer calibration by means of laser plasma. Spectrochim Acta Part B 178:106144
25. Oliver GD, Milton HT, Grisard JW (1953) The vapor pressure and critical constants of uranium hexafluoride. J Am Chem Soc 75:2827–2829
26. Peruski KM, Davis TA, Chan GCY, Mao XL, Trowbridge LD, Martin LR (Dec 2021) Cell design for laser-induced breakdown spectroscopy measurments on reactive gas samples. J Fluorine Chem:Under revision
27. Harrison GR, Loewen EG, Wiley RS (1976) Echelle gratings: Their testing and improvement. Appl Opt 15:971–976
28. Saunderson JL (1960) A method of uranium isotope analysis by direct reading emission spectroscopy. Talanta 6:63–70
29. Rossi G, Mol M (1969) Isotopic analysis of uranium by an optical spectral method—III: Determination of U235/U238 ratios with a hollow-cathode source and a direct-reading attachment. Spectrochim Acta Part B 24:389–398
30. Hainski Z, Rossi G (1965) Isotopic analysis of uranium by an optical spectral method – I. Determination of U235 in natural and depleted uranium with DC arc excitation and photographic recording. Energia Nucleare 12:306–309
31. Leys JA, Perkins RE (1966) Uranium isotope analysis by optical emission spectrometry. Anal Chem 38:1099–1101
32. El Sherbini AM, El Sherbini TM, Hegazy H, Cristoforetti G, Legnaioli S, Palleschi V, Pardini L, Salvetti A, Tognoni E (2005) Evaluation of self-absorption coefficients of aluminum emission lines in laser-induced breakdown spectroscopy measurements. Spectrochim Acta Part B 60:1573–1579
33. Cristoforetti G, Tognoni E (2013) Calculation of elemental columnar density from self-absorbed lines in laser-induced breakdown spectroscopy: a resource for quantitative analysis. Spectrochim Acta Part B 79–80:63–71
34. Takahashi T, Thornton B (2017) Quantitative methods for compensation of matrix effects and self-absorption in laser induced breakdown spectroscopy signals of solids. Spectrochim Acta Part B 138:31–42
35. Rezaei F, Cristoforetti G, Tognoni E, Legnaioli S, Palleschi V, Safi A (2020) A review of the current analytical approaches for evaluating, compensating and exploiting self-absorption in laser induced breakdown spectroscopy. Spectrochim Acta Part B 169:105878
36. International Atomic Energy Agency (IAEA) (2010) International target values 2010 for measurement uncertainties in safeguarding nuclear materials (STR-368), IAEA
37. Palmer BA, Engleman RJ, Keller RA (1980) An atlas of uranium emission intensities in a hollow-cathode discharge (LA-8251-MS), Los Alamos National Laboratory
38. Payling R, Larkins P (2000) Optical emission lines of the elements. Wiley, UK
39. Akaoka K, Oba M, Miyabe M, Otobe H, Wakaida I (2015) Measurement of uranium spectrum using laser induced breakdown spectroscopy – high resolution spectroscopy (350–470 nm) (JAEA-Research 2015–012), Japan Atomic Energy Agency
40. Akaoka K, Oba M, Miyabe M, Otobe H, Wakaida I (2016) Measurement of uranium spectrum using laser induced breakdown spectroscopy – high resolution spectroscopy (470–670 nm) (JAEA-Research 2016–005), Japan Atomic Energy Agency
41. Richards EWT, Crew MD (1959) The uranium spectrum between 3500 Å and 5500 Å with associated isotopic shifts (AERE-R-2941), United Kingdom Atomic Energy Authority
42. Smith DD (1952) Isotope spectrum shift data on uranium spectrum lines (ORNL-1412), Oak Ridge National Laboratory
43. Blaise J, Radziemski LJ (1976) Energy-levels of neutral atomic uranium (U I). J Opt Soc Am 66:644–659
44. Blaise J, Wyart JF, Verges J, Engleman R, Palmer BA, Radziemski LJ (1994) Energy-levels and isotope shifts for singly ionized uranium (U II). J Opt Soc Am B 11:1897–1929
45. Hou JJ, Zhang L, Zhao Y, Ma WG, Dong L, Yin WB, Xiao LT, Jia ST (2019) Resonance/non-resonance doublet-based self-absorption-free LIBS for quantitative analysis with a wide measurement range. Opt Express 27:3409–3421
46. Subramanian J, Simon R (2013) Overfitting in prediction models – is it a problem only in high dimensions? Contemp Clin Trials 36:636–641
47. Lever J, Krzywinski M, Altman N (2016) Model selection and overfitting. Nat Meth 13:703–704
48. Lefebvre-Brion H, Field RW (2004) Chapter 4 - methods of deperturbation. In: Lefebvre-Brion H, Field RW (eds) The spectra and dynamics of diatomic molecules. Academic Press, San Diego, pp 233–274
49. Motulsky HJ, Brown RE (2006) Detecting outliers when fitting data with nonlinear regression - a new method based on robust nonlinear regression and the false discovery rate. BMC Bioinf 7:123–123
50. Minguzzi P (2001) Some practical tools for everyday least squares. J Mol Spectrosc 209:169–177
51. Reed BC (2015) Straight-line fits with uncertainties in both coordinates: from Gauss to spreadsheets. Phys Scr 90:128001
52. Taylor PDP, Schutyser P (1986) Weighted linear regression applied in inductively coupled plasma-atomic emission spectrometry—a review of the statistical considerations involved. Spectrochim Acta Part B 41:1055–1061

53. Garden JS, Mitchell DG, Mills WN (1980) Nonconstant variance regression techniques for calibration-curve-based analysis. Anal Chem 52:2310–2315
54. Almeida AM, Castel-Branco MM, Falcão AC (2002) Linear regression for calibration lines revisited: weighting schemes for bioanalytical methods. J Chromatogr B 774:215–222

Journal : **Large 10967**	Article No : **8215**	Pages : **13**	MS Code : **8215**	Dispatch : **2-2-2022**